Preparation, structure and properties of three $[Mo_xW_{4−x}S_4(H_2O)_{12}]^{5+}$ (x = 1–3) and $[MoW_3Se_4(H_2O)_{12}]^{5+}$ cuboidal complexes alongside $[Mo_4S_4(H_2O)_{12}]^{5+}$ and $[Mo_4Se_4(H_2O)_{12}]^{5+}$

Iain J. McLean,[a] Rita Hernandez-Molina,[a] Maxim N. Sokolov,[a,b] Mi-Sook Seo,[a]
Alexander V. Virovets,[b] Mark R. J. Elsegood,[a] William Clegg[a] and A. Geoffrey Sykes*,[a]

[a] *Department of Chemistry, The University of Newcastle, Newcastle upon Tyne, UK NE1 7RU*
[b] *Institute of Inorganic Chemistry, Russian Academy of Sciences, pr Lavrentjeva 3,
Novosibirsk 630090, Russia*

The preparation of $[MoW_3S_4(H_2O)_{12}]^{5+}$, $[Mo_2W_2S_4(H_2O)_{12}]^{5+}$, $[Mo_3WS_4(H_2O)_{12}]^{5+}$ and $[MoW_3Se_4(H_2O)_{12}]^{5+}$ from trinuclear incomplete cuboidal complexes $[W_3S_4(H_2O)_9]^{4+}$, $[MoW_2S_4(H_2O)_9]^{4+}$, $[Mo_2WS_4(H_2O)_9]^{4+}$ and $[W_3Se_4(H_2O)_9]^{4+}$ respectively has been achieved by reaction with $[Mo_2Cl_8]^{4−}$. The structures of the 5+ cube $[MoW_3S_4(H_2O)_{12}][pts]_5 \cdot Hpts \cdot 16H_2O$ (pts$^−$ = p-toluenesulfonate) and $[Me_2NH_2]_6[MoW_3S_4(NCS)_{12}] \cdot 0.5H_2O$ (6+ cube) have been determined by X-ray diffraction. Reversible behaviour is observed in cyclic voltammetry on the 5+ cubes, and reduction potentials ($E^{\circ\prime}$ *vs.* NHE) for the 6+/5+ and 5+/4+ couples have been determined. The cubes are more strongly reducing as the number of W atoms is increased with $E^{\circ\prime}$/mV values for $[MoW_3S_4(H_2O)_{12}]^{6+/5+}$ (258), $[MoW_3S_4(H_2O)_{12}]^{5+/4+}$ (−395) significantly smaller than values previously reported for $[Mo_4S_4(H_2O)_{12}]^{6+/5+}$ (860) and $[Mo_4S_4(H_2O)_{12}]^{5+/4+}$ (210). Peaks λ/nm (ε/M$^{−1}$ cm$^{−1}$ per cube) from UV/VIS/NIR spectra in 2.0 M Hpts shift from 635(435), 1100(122) for $[Mo_4S_4(H_2O)_{12}]^{5+}$ to higher energy transitions at 522(660), 850(200) for $[MoW_3S_4(H_2O)_{12}]^{5+}$. Oxidation of the 5+ cubes with for example $[Fe(H_2O)_6]^{3+}$ gives first the 6+ cube which then decays with fragmentation to trinuclear products always with loss of W. While oxidation to the 6+ cube depends on reduction potentials, a different order is observed and other factors are important in the decay process.

Distinctive properties of the $[Mo_4S_4(H_2O)_{12}]^{5+}$ cube include its well-defined redox chemistry, and the existence of two other oxidation states $[Mo_4S_4(H_2O)_{12}]^{4+}$ and $[Mo_4S_4(H_2O)_{12}]^{6+}$.[1] These different states can be accessed by cyclic voltammetry as well as controlled redox interconversions. The 4+ Mo$^{III}_4$ cube has 12 electrons, sufficient for six metal–metal bonds, but is readily air oxidised to the 5+ ion.[2] In aqueous solution the 5+ cube (11e$^−$) is the most readily accessed, and most extensively studied, while the 6+ cube (10e$^−$) has a tendency to fragment due to its high charge and/or low electron count.[3] In contrast ≈20 Group 6 to Group 15 heteroatom (M′) derivatives of $[Mo_3S_4(H_2O)_9]^{4+}$, having single Mo$_3$M′S$_4$ or related double cube core structures, give no reversible electrochemistry,[4] and with one exception (that of M′ = Cu)[5] have only the one oxidation state which reverts in air to $[Mo_3S_4(H_2O)_9]^{4+}$. Although crystal structures of cuboidal $[W_4S_4\{S_2P(OEt)_2\}_6]$, $[W_4Se_4(CN)_{12}]^{6−}$ (both 6+ cubes), and the W$^V_4$ p-tolyl imido cube $[W_4S_4(tolN)_4\{S_2P(OEt)_2\}_4]$ have been described,[6–8] no preparations of $[W_4S_4(H_2O)_{12}]^{n+}$ cubes n = 4, 5 or 6 have yet been reported, and W$_4$S$_4$ cubes remain comparatively rare. In this paper we report the preparation of $[Mo_xW_{4−x}S_4(H_2O)_{12}]^{5+}$ (x = 1–3) cubes. A key question is whether there is a well-defined redox chemistry involving three oxidation states, as in the case of $[Mo_4S_4(H_2O)_{12}]^{5+}$, or whether properties are more like those of the heteroatom derivatives. Crystal structures of $[Mo_4S_4(H_2O)_{12}][pts]_5 \cdot 14H_2O$ (Hpts = p-toluenesulfonic acid),[9] $[Mo_4S_4(NH_3)_9]Cl_4 \cdot 7H_2O$,[10] and different salts of $[Mo_4S_4(edta)_2]^{2−,3−,4−}$ have been reported.[11] The corresponding selenium clusters $[Mo_4Se_4(H_2O)_{12}]^{n+}$ (n = 4–6) have been prepared, and a crystal structure of $[Mo_4Se_4(H_2O)_{12}][pts]_5 \cdot 14H_2O$ and other properties reported.[12,13]

Experimental

Preparation of starting materials

The polymeric compounds $\{W_3S_7Br_4\}_x$ and $\{W_3Se_7Br_4\}_x$ were first obtained by heating W, S (or Se) and Br$_2$ together in a sealed quartz tube.[14] Preparation of $[W_3S_4(H_2O)_9]^{4+}$ and $[W_3Se_4(H_2O)_9]^{4+}$ involved heating the appropriate polymeric compound (1 g) on a steam bath (≈90 °C) with excess H$_3$PO$_2$ (2 mL; 50% w/w in H$_2$O) in concentrated HCl (20 mL) for 15 h.[15–17] The product was diluted two-fold and filtered to remove any unreacted solid, diluted to 0.2 M HCl and loaded onto a Dowex 50W-X2 cation exchange column, final elution with 2 M HCl or 2 M Hpts.[18,19] The purple $[W_3S_4(H_2O)_9]^{4+}$ product was characterised by its UV/VIS absorbance spectrum,[18] peak positions λ/nm (ε/M$^{−1}$ cm$^{−1}$ per W$_3$) at 317 (6100), 570 (480) in 2 M HCl, and 315 (8650), 560 (546) in 2 M Hpts. A similar procedure was used to prepare green $[W_3Se_4(H_2O)_9]^{4+}$ characterised by peak positions 359 (6600), 618 nm (547 M$^{−1}$ cm$^{−1}$) in 2 M Hpts, and 360 (6950), 625 nm (500 M$^{−1}$ cm$^{−1}$) in 2 M HCl.[18]

To prepare $[Mo_2WS_4(H_2O)_9]^{4+}$ and $[MoW_2S_4(H_2O)_9]^{4+}$, NaBH$_4$ (3 g in 20 mL H$_2$O) and 6 M HCl (20 mL) were slowly added (30 min) to a solution of ammonium tetrasulfido-tungstate(VI), $[NH_4]_2[WS_4]$ (1 g),[20] and the Mo$^V_2$–cysteine complex Na$_2[Mo_2O_2(\mu$-S$)_2$(Cys$)_2] \cdot 4H_2O$ (1.87 g)[21] in H$_2$O (50 mL), as previously described.[22,23] After addition of further HCl (6 M, 80 mL) the solution was heated in a conical flask on a steam bath (≈90 °C) for 5 h in air. After cooling, the green-brown solution was filtered, loaded onto a G10 Sephadex column (90 × 4 cm), and eluted with 1.0 M HCl (>500 mL). Grey $[MoW_2S_4(H_2O)_9]^{4+}$ and green $[Mo_2WS_4(H_2O)_9]^{4+}$ bands were separated, and were further purified by Dowex 50W-X2 cation-exchange chromatography. The UV/VIS peak positions λ/nm (ε/M$^{−1}$ cm$^{−1}$ per trinuclear cluster) in 2 M Hpts were close to those previously reported in 2 M HClO$_4$; for $[Mo_2WS_4(H_2O)_9]^{4+}$ 340 (4390), 490 (sh) (298), 590 (322) and for $[MoW_2S_4(H_2O)_9]^{4+}$ 325 (5420), 490 (sh) (320), 570 (363).

Trinuclear $[Mo_3S_4(H_2O)_9]^{4+}$ formed as a decay product in some of the reactions considered herein has UV/VIS peak positions λ/nm (ε/M$^{−1}$ cm$^{−1}$ per Mo$_3$) at 370 (4995), 616 (326) in 2 M HCl, and 366 (5550), 603 (362) in 2 M Hpts.[22]

Table 1 Peak positions λ/nm (ε/M^{-1} cm^{-1} per cube) in the UV/VIS/NIR spectra of $[Mo_xW_{4-x}S_4(H_2O)_{12}]^{5+}$ and $[MoW_3Se_4(H_2O)_{12}]^{5+}$ alongside values previously reported for $[Mo_4S_4(H_2O)_{12}]^{5+}$ and $[Mo_4Se_4(H_2O)_{12}]^{5+}$ in 2.0 M Hpts. Values in 2 M HCl indicated in footnotes

5+ Cube	Colour	λ/nm (ε/M^{-1} cm^{-1} per cube)	Ref.
$[MoW_3S_4(H_2O)_{12}]^{5+}$	Orange-brown	522 (660); 850 (200) [a]	This work
$[Mo_2W_2S_4(H_2O)_{12}]^{5+}$	Pink-grey	560 (534); 1020 (168) [b]	This work
$[Mo_3WS_4(H_2O)_{12}]^{5+}$	Green (-blue)	611 (499); 1038 (188) [c]	This work
$[Mo_4S_4(H_2O)_{12}]^{5+}$	Green	635 (435); 1100 (122)	1
$[MoW_3Se_4(H_2O)_{12}]^{5+}$	Brown-orange	514 (sh) (690); 874 (160) [d]	This work
$[Mo_4Se_4(H_2O)_{12}]^{5+}$	Green	425 (sh) (669); 662 (407); 1188 (117)	12

[a] 522 (694); 857 (284). [b] 563 (502); 1000 (201). [c] 606 (457); 1040 (150). [d] 524 (769); 882 (172).

A sample of the purple-red octachlorodimolybdate(II) complex $K_4[Mo_2Cl_8]\cdot2H_2O$ was obtained by reacting tetra-μ-acetatodimolybdenum(II) $[Mo_2(O_2CCH_3)_4]$ with concentrated HCl as described.[24]

Other reagents

Sodium tetrahydroborate, $NaBH_4$; hypophosphorous acid (50% w/w solution in H_2O); white crystalline 98.5% p-toluenesulfonic acid (Hpts) as the monohydrate; 37% HCl AR grade; sodium thiocyanate; were all as obtained from Aldrich. Solutions of $[Fe(H_2O)_6]^{3+}$ were obtained by loading $Fe(ClO_4)_3$ (Fluka) onto a Dowex 50W-X2 cation-exchange column, and after washing with more dilute acid eluting with 1.0 M HCl or Hpts as required. The reduction potential of the $[Fe(H_2O)_6]^{3+/2+}$ couple vs. NHE is 770 mV.[25]

X-Ray crystallography

Crystal data for $[MoW_3S_4(H_2O)_{12}][pts]_5\cdot Hpts\cdot16H_2O$: $C_{42}H_{103}MoO_{46}S_{10}W_3$, $M = 2312.3$, monoclinic, $a = 13.8310(7)$, $b = 31.0531(17)$, $c = 19.7278(10)$ Å, $\beta = 110.311(2)°$, $U = 7946.2(7)$ Å^3, $T = 160$ K, space group $C2/c$, $Z = 4$, μ(Mo-Kα) = 4.84 mm^{-1}, 29 322 reflections measured (Bruker AXS SMART CCD diffractometer), 9508 unique ($R_{int} = 0.0372$) which were all used in refinement. Restraints were applied to disordered pts anions and water molecules. The final $wR(F^2)$ was 0.0762, with conventional $R = 0.0303$ ($F^2 > 2\sigma$).

Crystal data for $[Me_2NH_2]_6[MoW_3S_4(NCS)_{12}]\cdot0.5H_2O$: $C_{24}H_{49}MoN_{18}O_{0.5}S_{16}W_3$, $M = 1758.3$, cubic, $a = 22.759(6)$ Å, $U = 11\,788(5)$ Å^3, $T = 293$ K, space group $Pa3$, $Z = 8$, μ(Mo-Kα) = 6.65 mm^{-1}, 5312 reflections measured (Enraf-Nonius CAD4 diffractometer), 2454 unique ($R_{int} = 0.0722$) which were all used in refinement. The final $wR(F^2)$ was 0.0646, with conventional $R = 0.0351$ ($F^2 > 2\sigma$).

CCDC reference number 186/1048.

See http://www.rsc.org/suppdata/dt/1998/2557/ for crystallographic files in .cif format.

UV/VIS/NIR spectrophotometry

Measurements were carried out on a Perkin-Elmer Lambda 9 instrument, which includes the NIR range, and a Shimadzu 2101PC.

Electrochemistry

Cyclic voltammetry experiments were carried out using EG & G equipment with a computer interfaced PAR Model 173 potentiostat and a glassy carbon working electrode. The $[Fe(CN)_6]^{3-}$–$[Fe(CN)_6]^{4-}$ couple in 0.10 M KCl (410 mV vs. NHE) was used as an internal reference. The changes were confirmed as 1e$^-$ reversible processes from square-wave voltammetry. From repeat determinations the reproducibility was ±6 mV.

ICP-AES analyses

Inductively coupled plasma atomic emission spectrometry elemental analyses were carried out on an ATI Unicam 701

Table 2 ICP-AES analyses (ppm) for $[Mo_xW_{4-x}S_4(H_2O)_{12}]^{5+}$ cubes ($x = 1$–3). A solution of $[Mo_3S_4(H_2O)_9]^{4+}$ was used to calibrate for S, which with normal standards gives values $\approx$10% too high

Cube	Ratios		
	Mo	W	E (=S or Se)
$[Mo_3WS_4(H_2O)_{12}]^{5+}$	3.0	1.1	4.0
$[Mo_2W_2S_4(H_2O)_{12}]^{5+}$	2.0	2.0	4.0
$[MoW_3S_4(H_2O)_{12}]^{5+}$	1.0	3.0	
$[MoW_3Se_4(H_2O)_{12}]^{5+}$	1.0	3.0	4.8

instrument. To calibrate for S a known sample of $[Mo_3S_4(H_2O)_9]^{4+}$ was used, otherwise (with normal standards) values for S were $\approx$10% too high.

Results

Preparation of Mo/W containing 5+ cubes

Identical procedures were used to convert trinuclear $[W_3S_4(H_2O)_9]^{4+}$, $[MoW_2S_4(H_2O)_9]^{4+}$, $[Mo_2WS_4(H_2O)_9]^{4+}$ into the cubes $[MoW_3S_4(H_2O)_{12}]^{5+}$, $[Mo_2W_2S_4(H_2O)_{12}]^{5+}$, $[Mo_3WS_4(H_2O)_{12}]^{5+}$ respectively. Typically an air-free solution of the trinuclear cluster (11 mM; 20 mL) in 2 M HCl was added to a 20-fold excess of $K_4[Mo_2Cl_8]$ (0.3 g) and the mixture heated for $\approx$3 h at 90 °C (steam bath). The product was diluted to 0.3 M acid and loaded onto an air-free Dowex 50W-X2 cation-exchange column (20 × 1 cm diameter). Excess $[Mo_2Cl_8]^{4-}$ was not held by the column. To obtain Hpts solutions washing was with 0.5 M Hpts (100 mL) and 1.0 M Hpts (80 mL) when two bands separated. Unreacted trinuclear cluster was eluted with 2 M Hpts, and the 5+ cube with 3 to 4 M Hpts as required. Elution was alternatively with 2 M HCl. Peak positions in UV/VIS/NIR absorbance spectra, Table 1, were quantified in terms of ε values assuming air oxidation to a trinuclear product of known spectrum, and confirmed using ICP analyses (Table 2). The four metal atoms in the 5+ products have an average oxidation state of 3.25, and the trinuclear clusters written here as M$^{IV}_3$ undergo reductive addition with Mo$^{II}_2$, e.g. equation (1). No unreacted

$$W_3S_4^{4+} + Mo^{II}_2 \longrightarrow MoW_3S_4^{5+} + [Mo^{III}] \qquad (1)$$

trinuclear starting complex was observed on columns, and yields were close to 100%.

A similar procedure was used to convert $[W_3Se_4(H_2O)_9]^{4+}$ into $[MoW_3Se_4(H_2O)_{12}]^{5+}$. The UV/VIS/NIR peak positions are included in Table 1.

Isolation and characterisation of crystalline products

Orange-brown crystals of $[MoW_3S_4(H_2O)_{12}]^{5+}$ were obtained from the most concentrated fraction from a Dowex column, eluted with 4 M Hpts, after $\approx$1 week at -20 °C. The UV/VIS spectrum of the mother-liquor corresponded to that of $[MoW_3S_4(H_2O)_{12}]^{5+}$. The ICP-AES analyses on a solution prepared from the crystals gave satisfactory W:Mo ratios, Table 2. After leaving over $Mg(ClO_4)_2$ for 3 d analyses were carried out {Found: C, 22.16, 22.45; H, 3.49, 3.63. Calc. for
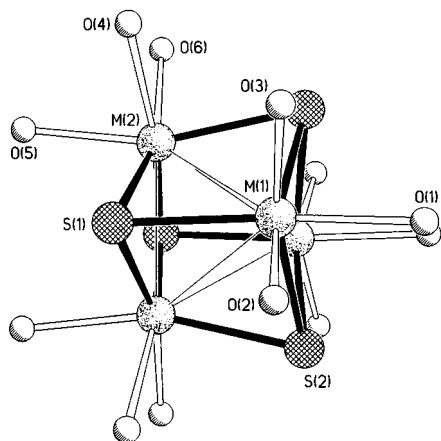
Fig. 1 Structure of the $[MoW_3S_4(H_2O)_{12}]^{5+}$ cation with unique atoms labelled. The cation lies on a two-fold rotation axis

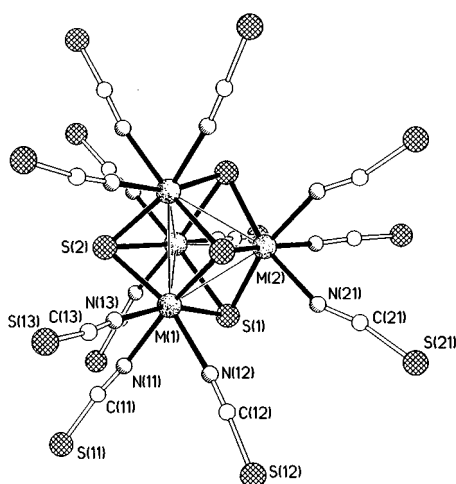**Fig. 2** Structure of the $[MoW_3S_4(NCS)_{12}]^{6-}$ anion with unique atoms labelled. The anion lies on a three-fold rotation axis through M(2) and S(2)

$C_{35}H_{59}MoO_{27}S_9W_3$: C, 22.74; H, 3.20%. Formula $[MoW_3S_4(H_2O)_{12}][pts]_5$}.

To a solution of $[W_3MoS_4(H_2O)_{12}]^{5+}$ in 2 M HCl solid NaNCS was added to ≈1 M. The colour changed to a dark red-brown in ≈20 min. A concentrated solution of Me_2NH_2Cl (5 mL) was added dropwise, and the solution left for 2 d in air. As in the case of $[Mo_4S_4(H_2O)_{12}]^{5+}$ air oxidation occurs in the presence of NCS^- giving the 6+ oxidation state.[1] The black crystals collected were analysed {Found: C, 16.37, 16.46; H, 2.58, 2.64; N, 14.09, 14.29. Calc. for $C_{24}H_{48}MoN_{18}S_{16}W_3$: C, 16.48; H, 2.77; N, 14.42%. Formula $[Me_2NH_2]_6[MoW_3S_4(NCS)_{12}]$}.

Crystal structures

Both structures contain complete M_4S_4 cubes with three terminal ligands (H_2O or NCS) on each metal atom, Figs. 1 and 2. Thiocyanate is co-ordinated through nitrogen. In both cases the Mo and W atoms are disordered over the four metal sites, representing random orientational disorder of the Mo_3WS_4 cubes. The counter ions and solvent water molecules also show disorder.

Selected geometric results are given in Tables 3 and 4. The M_4S_4 central units have M–S distances ranging from 2.3437(10) to 2.3836(12) Å in the aqua case, and 2.342(4) to 2.369(4) Å in the thiocyanate case. The M–M distances range from 2.7052(4) to 2.8793(3) Å (aqua) and 2.3814(14) to 2.8494(13) Å (thiocyanate). These are similar to corresponding distances found in the few other reported M_4S_4 cubes with exclusively aqua [26,27] or thiocyanato [28] ligands.

Table 3 Selected bond lengths (Å) and angles (°) for $[MoW_3S_4(H_2O)_{12}]$[pts]$_5$·Hpts·16H$_2$O

M(1)–M(2)	2.7650(3)	M(1)–M(1A)	2.8393(4)
M(1)–M(2A)	2.8793(3)	M(2)–M(2A)	2.7052(4)
M(1)–S(1)	2.3611(10)	M(1)–S(2)	2.3607(10)
M(1)–S(2A)	2.3437(10)	M(2)–S(1)	2.3486(12)
M(2)–S(1A)	2.3836(12)	M(2)–S(2A)	2.3673(10)
M(1)–O(1)	2.144(3)	M(1)–O(2)	2.148(3)
M(1)–O(3)	2.128(3)	M(2)–O(4)	2.125(3)
M(2)–O(5)	2.154(3)	M(2)–O(6)	2.181(3)
O(3)–M(1)–O(1)	80.65(10)	O(3)–M(1)–O(2)	77.53(11)
O(1)–M(1)–O(2)	79.17(10)	S(2A)–M(1)–S(2)	104.08(3)
S(2A)–M(1)–S(1)	106.67(4)	S(2)–M(1)–S(1)	101.55(4)
O(4)–M(2)–O(5)	81.11(11)	O(4)–M(2)–O(6)	78.79(11)
O(5)–M(2)–O(6)	80.29(11)	S(1)–M(2)–S(2A)	106.31(4)
S(1)–M(2)–S(1A)	108.64(4)	S(2A)–M(2)–S(1A)	100.70(4)
M(2)–S(1)–M(1)	71.90(3)	M(2)–S(1)–M(2A)	69.73(3)
M(1)–S(1)–M(2A)	74.72(3)	M(1A)–S(2)–M(1)	74.25(3)
M(1A)–S(2)–M(2A)	71.88(3)	M(1)–S(2)–M(2A)	75.03(3)

Symmetry transformations used to generate equivalent atoms: A $-x + 1, y, -z + \frac{1}{2}$; B $-x, -y, -z$.

Table 4 Selected bond lengths (Å) and angles (°) for $[Me_2NH_2]_6$-$[MoW_3S_4(NCS)_{12}]$·0.5H$_2$O

M(1)–M(2)	2.8494(13)	M(1)–M(1A)	2.8314(14)
M(1)–S(1)	2.369(4)	M(1)–S(1A)	2.363(4)
M(1)–S(2)	2.342(4)	M(2)–S(1)	2.356(4)
M(1)–N(11)	2.101(11)	M(1)–N(12)	2.090(12)
M(1)–N(13)	2.078(11)	M(2)–N(21)	2.08(2)
N(13)–M(1)–N(12)	82.0(5)	N(13)–M(1)–N(11)	81.3(5)
N(12)–M(1)–N(11)	80.2(5)	S(2)–M(1)–S(1A)	104.21(11)
S(2)–M(1)–S(1)	104.00(11)	S(1A)–M(1)–S(1)	103.4(2)
N(21)–M(2)–N(21A)	84.5(5)	S(1)–M(2)–S(1A)	103.95(10)
M(2)–S(1)–M(1B)	74.27(10)	M(2)–S(1)–M(1)	74.17(11)
M(1B)–S(1)–M(1)	73.50(11)	M(1A)–S(2)–M(1)	74.4(2)

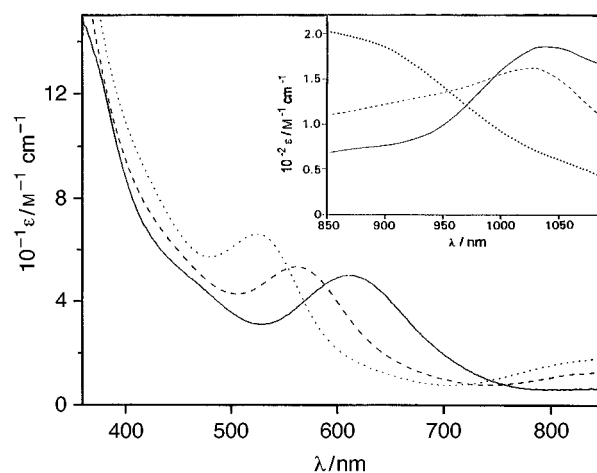Symmetry transformations used to generate equivalent atoms: A z, x, y; B y, z, x.

Fig. 3 The UV/VIS/NIR spectra of $[Mo_3WS_4(H_2O)_{12}]^{5+}$ (——), $[Mo_2W_2S_4(H_2O)_{12}]^{5+}$ (– – –) and $[MoW_3S_4(H_2O)_{12}]^{5+}$ (·····), in 2.0 M Hpts

Other characterisations of $[Mo_xW_{4-x}S_4(H_2O)_{12}]^{5+}$

The ICP-AES elemental analyses on 2.0 M HCl solutions are summarised in Table 2. The UV/VIS/NIR spectra for $[Mo_xW_{4-x}S_4(H_2O)_{12}]^{5+}$ are shown in Fig. 3 and those for $[MoW_3Se_4(H_2O)_{12}]^{5+}$ and $[MoW_3S_4(H_2O)_{12}]^{5+}$ in Fig. 4, with a listing of peak positions alongside those for $[Mo_4S_4(H_2O)_{12}]^{5+}$ in Table 1.[1,12] In all cases spectra and redox properties are consistent with products in the 5+ state. Peak positions shift to

Table 5 Reduction potentials $E^{\circ\prime}$ vs. NHE ($\approx 20\,°C$) from cyclic and square-wave voltammetry on $[Mo_xW_{4-x}S_4(H_2O)_{12}]^{5+}$ and $[MoW_3Se_4(H_2O)_{12}]^{5+}$ alongside values previously determined for $[Mo_4S_4(H_2O)_{12}]^{5+}$ and $[Mo_4Se_4(H_2O)_{12}]^{5+}$ in 2.0 M Hpts. The $E_1^{\circ\prime}$ values are for the 6+/5+ couples, and $E_2^{\circ\prime}$ for the 5+/4+ couples

5+ Cube	$E_1^{\circ\prime}$/mV	$E_2^{\circ\prime}$/mV	Ref.
$[MoW_3S_4(H_2O)_{12}]^{5+}$	258	−395	This work
$[Mo_2W_2S_4(H_2O)_{12}]^{5+}$	422	−248	This work
$[Mo_3WS_4(H_2O)_{12}]^{5+}$	673	6	This work
$[Mo_4S_4(H_2O)_{12}]^{5+}$	860	210	1
$[MoW_3Se_4(H_2O)_{12}]^{5+}$	214	−410	This work
$[Mo_4Se_4(H_2O)_{12}]^{5+}$	792	193	12
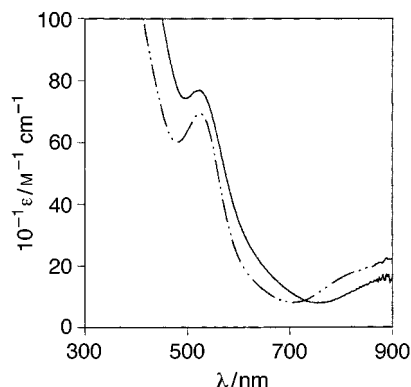
Fig. 4 The UV/VIS/NIR spectrum of $[MoW_3Se_4(H_2O)_{12}]^{5+}$ (——) alongside that of $[MoW_3S_4(H_2O)_{12}]^{5+}$ (–··–) in 2.0 M HCl
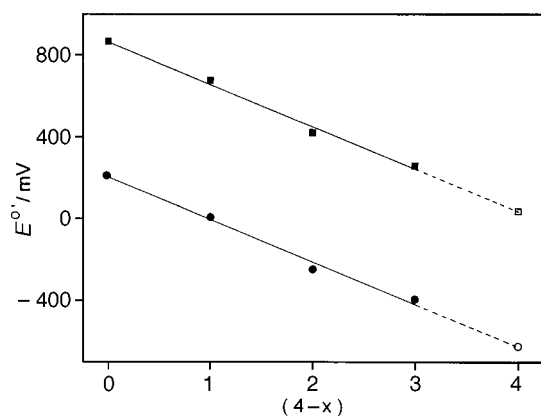
Fig. 5 Variation of reduction potentials vs. NHE ($\approx 20\,°C$), $E_1^{\circ\prime}$ for $[Mo_xW_{4-x}S_4(H_2O)_{12}]^{6+/5+}$ and $E_2^{\circ\prime}$ for $[Mo_xW_{4-x}S_4(H_2O)_{12}]^{5+/4+}$ couples ($x = 1$–3), from cyclic voltammetry in 2.0 M Hpts solutions alongside those for the corresponding Mo_4S_4 ($x = 4$) couples.[1] The open circles are extrapolated values for the W_4S_4 ($x = 0$) cubes which have not so far been isolated

higher energy (lower λ) values on increasing the number of W atoms.

Electrochemical studies on $[Mo_xW_{4-x}S_4(H_2O)_{12}]^{5+}$ cubes

Reversible oxidation and reduction processes were observed for the $x = 1$–3 cubes. Solutions were O_2-free (N_2 used). Reduction potentials $E^{\circ\prime}$ vs. NHE for the 6+/5+ ($E_1^{\circ\prime}$) and 5+/4+ ($E_2^{\circ\prime}$) couples (2) and (3) were determined. These increase as x

$$Mo_xW_{4-x}S_4^{6+} + e^- \rightleftharpoons Mo_xW_{4-x}S_4^{5+} \qquad (2)$$

$$Mo_xW_{4-x}S_4^{5+} + e^- \rightleftharpoons Mo_xW_{4-x}S_4^{4+} \qquad (3)$$
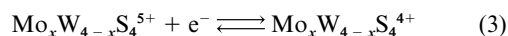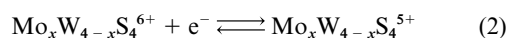
increases, Table 5. Values of $E^{\circ\prime}$ for $[Mo_4S_4(H_2O)_{12}]^{5+}$ have been reported previously, and are also included.[1] Graphs showing linear trends of $E^{\circ\prime}$ with $4 - x$ are shown in Fig. 5. From
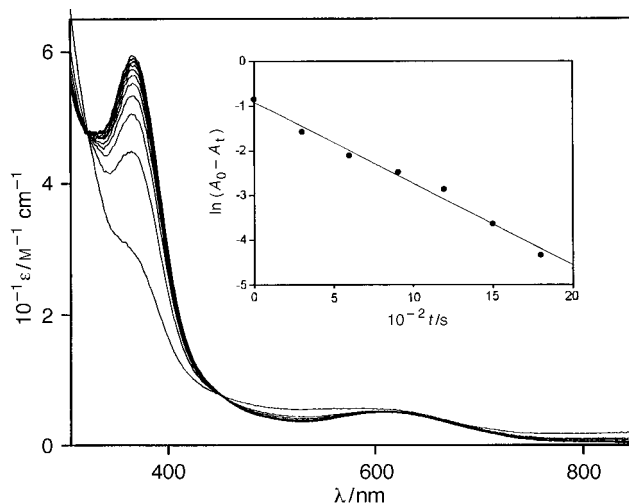

Fig. 6 The UV/VIS absorbance spectra for the reaction of $[Mo_3WS_4(H_2O)_{12}]^{5+}$ (≈ 0.3 mM) with $[Fe(H_2O)_6]^{3+}$ (≈ 2.1 mM) at 25 °C in 2.0 M Hpts recorded at 5 min intervals (absorbance increases at ≈ 350 nm). The first spectrum is for $[Mo_3WS_4(H_2O)_{12}]^{6+}$, and the kinetic first-order plot (inset) is for the decay of this species

these values it would be expected that rate constants for the oxidation of 5+ cubes to 6+ would decrease as x increases.

Characterisation of $[MoW_3Se_4(H_2O)_{12}]^{5+}$

The product was eluted with 2 M HCl from a Dowex 50W-X2 column and reacted with excess NCS$^-$ (≈ 1 M). Black crystals of $[Me_2NH_2]_6[MoW_3Se_4(NCS)_{12}]$ were obtained (Found: C, 14.72; H, 2.10; N, 12.55. Calc. for $C_{24}H_{48}MoN_{18}S_{12}Se_4W_3$: C, 14.88; H, 2.55; N, 13.02%). Details of the UV/VIS/NIR spectrum along with those for the $[Mo_4Se_4(H_2O)_{12}]^{5+}$ and ICP analyses on a 2 M HCl solution are included in Tables 1 and 2. Reduction potentials are listed in Table 5.

Double cube products

In the column chromatography carried out to isolate $[MoW_3S_4(H_2O)_{12}]^{5+}$ small amounts of a violet more highly charged product eluted with 4 M Hpts, and gave a UV/VIS absorption spectrum with peaks/nm at 440, 569 and 831. Similarly in the corresponding $[MoW_3Se_4(H_2O)_{12}]^{5+}$ preparation a violet product was obtained with peaks at 446, 557 and 818 nm. The latter gave ICP-AES analyses W:Mo:Se of 6.0:1.4:7.4. Together with the elution behaviour and shape of UV/VIS spectra, the products are believed to be the corner-shared double cubes $[MoW_6S_8(H_2O)_{18}]^{8+}$ and $[MoW_6Se_6(H_2O)_{18}]^{8+}$, analogues of the previously reported $[Mo_7S_8(H_2O)_{18}]^{8+}$ and $[Mo_7Se_8(H_2O)_{18}]^{8+}$.[29]

Stability of $[Mo_xW_{4-x}S_4(H_2O)_{12}]^{5+}$ in air

Air oxidation of the $x = 1$–3 cubes ($\approx 9 \times 10^{-4}$ M) in 2.9 M Hpts was monitored by UV/VIS absorbance changes in the 500–600 nm range. Overall rates were not in the order expected from $E^{\circ\prime}$ values, and at least two stages are observed. Trinuclear products were obtained. For example in the case of $[Mo_3WS_4(H_2O)_{12}]^{5+}$ reaction is complete overnight to give $[Mo_3S_4(H_2O)_9]^{4+}$. Solutions of $[Mo_2W_2S_4(H_2O)_{12}]^{5+}$ and $[MoW_3S_4(H_2O)_{12}]^{5+}$ give first a brown coloration believed to be the corresponding 6+ cubes which decay over longer periods to give respectively green $[Mo_2WS_4(H_2O)_9]^{4+}$ (2–3 d), and grey $[MoW_2S_4(H_2O)_9]^{4+}$ (≈ 1 week). The trinuclear products are formed in a process which involves exclusively loss of W.

Oxidation of $[Mo_xW_{4-x}S_4(H_2O)_{12}]^{5+}$ with $[Fe(H_2O)_6]^{3+}$

Reactions of the $x = 1$–3 cubes (≈ 0.3 mM) with a seven-fold excess of $[Fe(H_2O)_6]^{3+}$ (≈ 2.1 mM) were monitored by UV/VIS spectrophotometry, e.g. Figs. 6 and 7. Two separate stages are
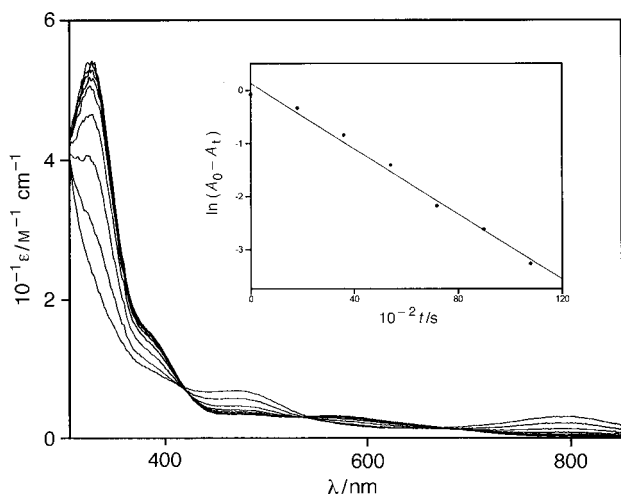
Fig. 7 The UV/VIS absorbance spectra for the reaction of $[MoW_3S_4(H_2O)_{12}]^{5+}$ (≈ 0.3 mM) with $[Fe(H_2O)_6]^{3+}$ (≈ 2.1 mM) at 25 °C, in 2.0 M Hpts recorded at 30 min intervals (absorbance increases at ≈ 350 nm). The first spectrum is for $[MoW_3S_4(H_2O)_{12}]^{6+}$, and the kinetic first-order plot (inset) is for the decay of this species

observed. The first spectrum obtained is that of the 6+ cube following rapid oxidation of the 5+ cube. Although no rate constants were determined rates observed for the first stage are according to $E_1^{\circ\prime}$ values with the $[MoW_3S_4(H_2O)_{12}]^{5+}$ cube reacting the fastest. The second stage corresponds to a slower decay process giving the same trinuclear product as in the air oxidation experiments. Thus the $[Mo_3WS_4(H_2O)_{12}]^{5+}$ cube is converted into $[Mo_3S_4(H_2O)_9]^{4+}$ (Fig. 6), and $[MoW_3S_4(H_2O)_{12}]^{5+}$ into $[MoW_2(H_2O)_9]^{4+}$ (Fig. 7), with loss of W in both cases. The decay of $[Mo_3WS_4(H_2O)_{12}]^{6+}$ ($k = 1.8 \times 10^{-3}$ s^{-1}), Fig. 6, is faster than the decay of $[MoW_3S_4(H_2O)_{12}]^{6+}$ ($k = 3.1 \times 10^{-4}$ s^{-1}), Fig. 7. After completion of the reaction a faint deposit formed on the side of the optical cell, and is most likely a polymeric film of W^{VI}. However, amounts (and conditions) were not suitable for tests using Sn^{II} (reductant generating W blues), or Ag$^+$ (yellow precipitate with $[WO_4]^{2-}$),[30] and we have been unable to confirm the identity of this product. Cross-over points in the early stages of the runs shift slightly, Figs. 6 and 7, due to some overlapping of the two stages. No reaction was observed for $[Mo_4S_4(H_2O)_{12}]^{5+}$ with $[Fe(H_2O)_6]^{3+}$ (20-fold excess), a process which is thermodynamically unfavourable by ≈ 90 mV.

Discussion

First some comment is required on the crystal structure and formula assigned to the 5+ cube $[MoW_3S_4(H_2O)_{12}][pts]_5\cdot$Hpts$\cdot16H_2O$. The mother-liquor from which crystals were obtained gave the UV/VIS spectrum of $[MoW_3S_4(H_2O)_{12}]^{5+}$. Crystals were moreover the orange-brown colour of the 5+ cube. The six pts$^-$ groups detected in the structure unit cell are therefore assigned as five pts$^-$ counter ions and one Hpts, and not six pts$^-$ which would imply a 6+ charge on the cube. It is difficult to distinguish between Hpts and pts$^-$ in the crystal structure because of extensive hydration and H-bonding involving pts$^-$ groups. Also with regard to the second crystal structure the cluster anion $[MoW_3S_4(NCS)_{12}]^{6-}$ is obtained by reacting $[MoW_3S_4(H_2O)_{12}]^{5+}$ in 2.0 M HCl with 1 M NCS$^-$ in air, when oxidation occurs. Such an oxidation of 5+ to 6+ has been observed previously for $[Mo_4S_4(H_2O)_{12}]^{5+}$ in the presence of 1 M NCS$^-$.[1,28] In both structures reported herein the Mo and W atoms are disordered. Metal–metal bonding is evident, but the precision is not sufficient to define differences in bond lengths for the 5+ and 6+ oxidation states.

The UV/VIS/NIR spectra of the three new Mo/W cubes in the 5+ state, Fig. 3, indicated prominent LMCT transitions.

Peak positions, alongside those for $[Mo_4S_4(H_2O)_{12}]^{5+}$,[1] are compared in Table 1. Wavelength (λ/nm) trends observed for the $Mo_4S_4^{5+}$, $Mo_3WS_4^{5+}$, $Mo_2W_2S_4^{5+}$, $MoW_3S_4^{5+}$ cores, 635$\rightarrow$611$\rightarrow$560$\rightarrow$522 and 1100$\rightarrow$1038$\rightarrow$1020$\rightarrow$850 indicate shifts to higher energy transitions with an increasing number of W atoms.

Reduction potentials (*vs.* NHE) for the 6+/5+ ($E_1^{\circ\prime}$) and 5+/4+ ($E_2^{\circ\prime}$) couples, Table 5, also show systematic trends to more negative values the more W atoms are incorporated. The linear plots in Fig. 5 indicate shifts of about equal increments for each W included. The shifts observed reflect the greater difficulty in generating the lower oxidation states of W. Such effects are now well documented. Thus the stronger preference of W (over Mo) for the higher oxidation states is demonstrated by the 10^5–10^6 times greater rate constants for the $[IrCl_6]^{2-}$ oxidation of dinuclear M$^V_2$ complexes $[W_2O_4(H_2O)_6]^{2+}$ *vs.* $[Mo_2O_4(H_2O)_6]^{2+}$,[31] and $[W_2O_4(edta)]^{2-}$ *vs.* $[Mo_2O_4(edta)]^{2-}$.[32] The same ratio applies also for the trinuclear M$^{IV}_3$ complex $[W_3O_4(H_2O)_9]^{4+}$ *vs.* $[Mo_3O_4(H_2O)_9]^{4+}$.[33] Although few reduction potentials have been reported for Mo and W couples respectively, from studies on Keggin heteropolyanions incorporating W and Mo it has been concluded that the W^{VI}/W^V couple is >400 mV more strongly reducing (the reduction potential is more negative) than the Mo^{VI}/Mo^V couple.[34] Latimer has also listed potentials for the WO$_3$(s)/W$_2$O$_5$ (30 mV) and MoO$_3$(aq)/MoO$_2^+$ (400 mV) couples.[25] In the present work the difference in $E^{\circ\prime}$ with incorporation of each W averages 205 mV. The E° values for $[MoW_3Se_4(H_2O)_{12}]^{5+}$ as compared with $[Mo_4Se_4(H_2O)_{12}]^{5+}$ show similar trends, Table 5. In view of the different redox properties of Mo and W it seems reasonable to regard the $[Mo_3WS_4(H_2O)_{12}]^{5+}$ cube as approximating to Mo$^{III}_3$W^{IV} oxidation states.[35,36] Other assignments such as Mo$^{III}_2$W^{III}W^{IV} for Mo$_2$W$_2$S$_4^{5+}$ suggest possible delocalisation of the two W's to give an average 3.5 oxidation state. With the 6+ cubes an assignment Mo$^{III}_2$W$^{IV}_2$ for Mo$_2$W$_2$S$_4^{6+}$ may be acceptable, but Mo$^{III}_3$W^V for Mo$_3$WS$_4^{6+}$ seems less likely because of the need to generate an oxo/hydroxo ligand to the W^V.

The UV/VIS spectrophotometric changes for the oxidation of $[Mo_xW_{4-x}S_4(H_2O)_{12}]^{5+}$ cubes with $[Fe(H_2O)_6]^{3+}$ indicate two stage processes with formation of 6+ cubes in the first stage. A decay to the trinuclear clusters is then observed. Relative rates of the first stage are determined by $E_1^{\circ\prime}$ values, Table 5, with $[MoW_3S_4(H_2O)_{12}]^{5+}$ predictably the fastest reaction. Stability of the 6+ cube is greater the more W atoms are present. The reaction sequence is illustrated as in equation (4),

$$MoW_3S_4^{5+} \xrightarrow{k_1} MoW_3S_4^{6+} \xrightarrow{k_2} MoW_2S_4^{4+} + [W] \quad (4)$$
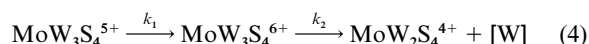
with k_1 largest and k_2 smallest for the $x = 1$ reaction shown. The reactions represent an efficient preparative route for the conversion of $[W_3S_4(H_2O)_9]^{4+}$ into $[MoW_2S_4(H_2O)_9]^{4+}$ *etc.*

No W$_4$S$_4$ core aqua ion has yet been prepared. Extrapolation of the correlations in Fig. 5 by linear regression method gives estimated reduction potentials for $[W_4S_4(H_2O)_{12}]^{6+/5+}$ of 39 mV, and for $[W_4S_4(H_2O)_{12}]^{5+/4+}$ of -627 mV, which are 821 mV and 837 mV respectively more negative than the corresponding values for the Mo$_4$S$_4$ cubes. The $[W_4S_4(H_2O)_{12}]^{6+}$ is therefore the most likely oxidation state to be generated, with $[W_4S_4(H_2O)_{12}]^{4+}$ much more difficult to access. Fragmentation of $[W_4S_4(H_2O)_{12}]^{6+}$ to give $[W_3S_4(H_2O)_9]^{4+}$ is a possible competing process. Existing W$_4$S$_4$ cubes have already been referred to,[6–8] and CN$^-$ is also expected to stabilise the different oxidation states.[37] It is possible to predict the UV/VIS peak positions for the $[W_4S_4(H_2O)_{12}]^{5+/6+}$ cubes from the information in Table 1 and Fig. 3.

In more general terms, variable oxidation state behaviour is observed for the Group 6 $[M_4S_4(H_2O)_{12}]^{n+}$ and $[M_4Se_4(H_2O)_{12}]^{n+}$ (M = Mo or W) mixed cubes considered in this paper ($n = 4$–6), and the chemistry is quite different to the higher electron count heteroatom (M') derivatives of $[Mo_3S_4(H_2O)_9]^{4+}$ and

$[W_3S_4(H_2O)_9]^{4+}$ obtained by incorporation of M′ from other (higher) groups up to 15. As far as structural properties (including bond lengths) are concerned Mo and W give very similar behaviour, and are interchangeable, even to the extent of giving corner-shared double cubes. In contrast striking differences in redox properties of Mo and W are illustrated in these studies.

Acknowledgements

References

1 B.-L. Ooi, C. Sharp and A. G. Sykes, *J. Am. Chem. Soc.*, 1989, **111**, 125.
2 C. Sharp and A. G. Sykes, *J. Chem. Soc., Dalton Trans.*, 1988, 2579.
3 M.-C. Hong, Y.-J. Li, J.-X. Lu, M. Nasreldin and A. G. Sykes, *J. Chem. Soc., Dalton Trans.*, 1993, 2613.
4 D. M. Saysell, M. N. Sokolov and A. G. Sykes, *ACS Symp. Ser.*, 1996, **653**, 216.
5 M. Nasreldin, Y.-J. Li, F. E. Mabbs and A. G. Sykes, *Inorg. Chem.*, 1994, **33**, 4283.
6 S.-F. Lu, J.-Q. Huang, H.-H. Zhuang, J.-Q. Li, D.-M. Wu and Z.-X. Xiang, *Polyhedron*, 1991, **10**, 2203.
7 M. L. Sampson, J. F. Richardson and M.E. Noble, *Inorg. Chem.*, 1992, **31**, 2726.
8 V. P. Fedin, I. V. Kalinia, A. V. Virovets, N. Y. Podbevezskaya and A. G. Sykes, *Chem. Commun.*, 1998, 237.
9 H. Akashi, T. Shibahara, T. Narahara, H. Tsuru and H. Kuroya, *Chem. Lett.*, 1989, 129.
10 T. Shibahara, E. Kawano, M. Okano, M. Nishi and H. Kuroya, *Chem. Lett.*, 1986, 827.
11 T. Shibahara, H. Kuroya, K. Matsumoto and S. Ooi, *Inorg. Chim. Acta*, 1986, **116**, L25.
12 M. Nasreldin, G. Henkel, G. Kampmann, B. Krebs, G. J. Lamprecht, C. A. Routledge and A. G. Sykes, *J. Chem. Soc., Dalton Trans.*, 1993, 737.
13 G. J. Lamprecht, M. Martinez, M. Nasreldin, C. A. Routledge, N. Al-Shatti and A. G. Sykes, *J. Chem. Soc., Dalton Trans.*, 1993, 747.
14 V. P. Fedin, M. N. Sokolov, O. A. Geras'ko, A. V. Virovets, N. V. Podberezskaya and V. Ye. Federov, *Inorg. Chim. Acta*, 1991, **187**, 81.
15 D. M. Saysell, V. P. Fedin, G. J. Lamprecht, M. N. Sokolov and A. G. Sykes, *Inorg. Chem.*, 1997, **36**, 2982.
16 V. P. Fedin, G. J. Lamprecht, T. Kohzuma, W. Clegg, M. R. J. Elsegood and A. G. Sykes, *J. Chem. Soc., Dalton Trans.*, 1997, 1747.
17 V. P. Fedin, M. N. Sokolov, A. V. Virovets, N. V. Podberezskaya and V. E. Federov, *Inorg. Chim. Acta*, 1998, **269**, 292.
18 R. Hernandez-Molina, D. N. Dybtsev, V. P. Fedin, M. R. J. Elsegood, W. Clegg and A. G. Sykes, *Inorg. Chem.*, 1998, **37**, 2995.
19 V. P. Fedin, M. N. Sokolov and A. G. Sykes, *J. Chem. Soc., Dalton Trans.*, 1996, 4089.
20 J. W. McDonald, G. D. Friesen, L. D. Rosenheim and W. E. Newton, *Inorg. Chim. Acta*, 1983, **72**, 205.
21 V. R. Ott, D. S. Sweiter and F. A. Schulz, *Inorg. Chem.*, 1977, **16**, 2538.
22 J. E. Varey and A. G. Sykes, *J. Chem. Soc., Dalton Trans.*, 1993, 3293.
23 T. Shibahara and M. Yamasaki, *Inorg. Chem.*, 1991, **30**, 1687, 1996, 4089.
24 J. V. Brencic and F. A. Cotton, *Inorg. Chem.*, 1970, **9**, 351.
25 W. M. Latimer, in *Oxidation States of the Elements and Their Potentials in Aqueous Solutions*, Prentice-Hall, Englewood Cliffs, NJ, 2nd edn., 1952.
26 T. Shibahara, T. Yamamoto, H. K. Kanadani and H. Kuroya, *J. Am. Chem. Soc.*, 1987, **109**, 3495.
27 T. Shibahara, H. Kuroya, H. Akashi, K. Matsumoto and S. Ooi, *Inorg. Chim. Acta*, 1993, **212**, 251.
28 F. A. Cotton, M. P. Diebold, Z. Dori, R. Llusar and W. Schwotzer, *J. Am. Chem. Soc.*, 1985, **107**, 6735.
29 M. N. Sokolov, N. Coichev, H. D. Moya, R. Hernandez-Molina, C. D. Borman and A. G. Sykes, *J. Chem. Soc., Dalton Trans.*, 1997, 1863.
30 A. E. Vogel and G. Svehla, 'Macro- and Semimicro Qualitative Inorganic Analyses', Longman, London, 5th edn. revised by G. Svehla, 1979.
31 C. Sharp, E. F. Hills and A. G. Sykes, *J. Chem. Soc., Dalton Trans.*, 1987, 2293; G. R. Cayley, R. S. Taylor, R. K. Wharton and A. G. Sykes, *Inorg. Chem.*, 1977, **16**, 1377.
32 A. B. Soares, R. C. Taylor and A. G. Sykes, *J. Chem. Soc., Dalton Trans.*, 1980, 1101; R. K. Wharton, J. F. Ojo and A. G. Sykes, *J. Chem. Soc., Dalton Trans.*, 1975, 1526.
33 B.-L. Ooi, A. L. Petrou and A. G. Sykes, *Inorg. Chem.*, 1988, **27**, 3626; B.-L. Ooi and A. G. Sykes, *Inorg. Chem.*, 1988, **27**, 310.
34 J. J. Altenau, M. T. Pope, R. A. Prados and H. So, *Inorg. Chem.*, 1975, **14**, 417.
35 Y.-J. Li, M. Nasreldin, M. Humanes and A. G. Sykes, *Inorg. Chem.*, 1992, **31**, 3011.
36 W. McFarlane, M. Nasreldin, D. M. Saysell, Z.-S. Jia, W. Clegg, M. R. J. Elsegood, K. S. Murray, B. Moubaraki and A. G. Sykes, *J. Chem. Soc., Dalton Trans.*, 1996, 363.
37 A. Müller, R. Jostes, W. Eltzner, C.-S. Nie, E. Diemann, H. Bögge, M. Zimmermann, M. Dartmann, U. Reinsch-Vogell, S. Che, S. J. Cyvin and B. N. Cyvin, *Inorg. Chem.*, 1985, **24**, 2872.